

States of ^{86}Rb : The $^{87}\text{Rb}(d, t)^{86}\text{Rb}$ Reaction*

J. E. Holden, J. J. Kolata, and W. W. Daehnick

Nuclear Physics Laboratory, University of Pittsburgh, Pittsburgh, Pennsylvania 15213

(Received 13 June 1972)

The states of ^{86}Rb were studied using the $^{87}\text{Rb}(d, t)^{86}\text{Rb}$ reaction at 17.5-MeV incident energy. Spectra were obtained using an Enge split-pole magnetic spectrograph; over-all energy resolution was 9 keV. Angular distributions were obtained from 9 to 60° laboratory angle for 25 levels up to 2 MeV excitation. Comparison with distorted-wave Born-approximation calculations yielded unique l -value assignments for 18 transitions; absolute spectroscopic factors were also extracted. Implications about the structure of the low-lying states are pointed out. The significant excitation of the $J^\pi = 2^-$ ground state of ^{86}Rb indicates weak $3s_{1/2}$ and $2d_{5/2}$ admixtures in the ^{87}Rb ground state.

I. INTRODUCTION

The interpretation of nuclei near $A=90$ in terms of a few particles outside a spherical and essentially inert ^{88}Sr or ^{90}Zr core has been quite successful. Over-all agreement between data and calculations remains good even up to nuclides having four particles outside of a ^{88}Sr core.¹ An interesting extension of this work would be the investigation of nuclei which can be interpreted as a few holes in this same core. ^{86}Rb is such a nucleus and hopefully most of its low-lying excitations can be described in terms of a proton hole and a neutron hole in ^{88}Sr , and the interactions between them. The hole states in ^{86}Rb have been studied in this laboratory by means of the (d, t) and (d, α) pickup reactions. The $^{87}\text{Rb}(d, t)^{86}\text{Rb}$ reaction is reported here. The $^{88}\text{Sr}(d, \alpha)^{86}\text{Rb}$ reaction is described in the following paper.² Interpretation of the (d, t) results in this article is chiefly spectroscopic; the structural implications of the (d, t) results are developed more fully in Ref. 2.

II. EXPERIMENTAL METHOD

The $^{87}\text{Rb}(d, t)^{86}\text{Rb}$ reaction was studied using a 17.5-MeV deuteron beam from the University of Pittsburgh three-stage tandem Van de Graaff accelerator. Details of the beam-transport system have been described elsewhere.³ The beam was focused through a 0.5-mm-wide by 2.0-mm-high collimating slit, placed 2 cm from the target; an antiscattering slit was placed between this slit and the target. The beam currents on both slits were monitored constantly throughout the experiment. Current on the defining slit was low enough to allow measurements to laboratory angles as low as 9°. The target was fabricated by the evaporation of $65 \mu\text{g}/\text{cm}^2$ of RbCl , enriched to 99.2% ^{87}Rb , onto a $30\text{-}\mu\text{g}/\text{cm}^2$ carbon backing. Tritons

were detected in nuclear emulsions located in the focal plane of an Enge split-pole spectrograph. The expected cross-section variation from state to state at a given angle was large, and two exposures were made at each angle, one of $1000\text{-}\mu\text{C}$ and one of $100\text{-}\mu\text{C}$ integrated beam charge.

The exposed plates were scanned at the Argonne automatic plate scanning facility.⁴ Spot checks of the automatic scanning were made by the Pittsburgh manual scanning group. In addition, the results from the two different exposures at each angle were used as a check of internal consistency. Agreement was very good within the known dynamic range of each scanning method. The regions near 0.78 and 1.1 MeV excitation were scanned manually at all angles to confirm the presence of weak groups in these regions.

The excitation energies tabulated in Table I were obtained from an internal calibration, using the following prescription. Six excited levels were chosen from the (d, t) spectra on the basis of their strength and general freedom from contaminants. In addition, these six levels were investigated for any possible doublet structure; in no case was any such evidence found. A spectrograph energy calibration was generated⁵ for each angle by using the energies found for these six levels in the (n, γ) work of Dawson, Sheline, and Jurney.⁶ Excitation energies were then computed for the remaining levels at all angles. The rms deviation of level energy measurements at all 13 angles was typically 2 keV, and agreement with the (n, γ) results⁶ and with the (d, α) results of Ref. 2 was excellent.

Relative normalization for the data was obtained by charge integration and by detecting elastically scattered deuterons in a pair of monitor $\text{NaI}(\text{Tl})$ detectors kept fixed at 38° throughout the experiment. The absolute normalization of the data was obtained by means of target thickness measurements using deuteron elastic scattering at 11.8

TABLE I. Summary of the results. The differential cross sections listed in the third column are those of the most forward maximum of the DWBA prediction giving the best over-all fit to the data. In the case of the levels at 0.0, 1.105, and 1.892 MeV, the cross sections are those of the DWBA predictions mixed to yield the solid curves of Figs. 4 and 5. The fourth column shows the neutron-pickup spectroscopic factors for each level. The $l=4$ factors listed were computed for $1g_{9/2}$ pickup. The $l=1$ factors listed are all for $2p_{3/2}$ pickup; those for $2p_{1/2}$ pickup would be 11% larger, independent of excitation energy.

E_x (MeV)	l_n	$\frac{d\sigma}{d\Omega}$ (mb/sr) _{max}	S_{lj}
0.0	{ 0	0.48	0.008
		0.11	0.025
0.489	1	4.2	0.59
0.556	4	1.35	4.6
0.872	4	0.29	1.1
0.977	4	0.58	2.3
1.027	1	4.34	0.78
1.091	4	0.61	2.5
1.105	{ 3	0.10	0.33
		0.06	0.011
1.122	1	0.37	0.006
1.156	1	0.69	0.13
1.195	...	0.20	...
1.245	4	0.048	0.21
1.304	1	0.17	0.035
1.389	1	1.01	0.22
1.412	4	0.14	0.64
1.438	...	0.13	...
1.470	1	1.35	0.31
1.500	1	0.33	0.077
1.547	4	0.058	0.28
1.668	1	4.5	1.15
1.708	1	1.12	0.29
1.762	1	0.80	0.22
1.892	{ 3	0.15	0.68
		0.12	0.034
1.919	...	0.10	...

and 17.5 MeV. The elastic scattering cross sections were taken from Mairle and Schmidt-Rohr⁷ for the 11.8-MeV case and from the optical-model prediction at 17.5 MeV using the parameters of Table II. The uncertainty in the absolute normalization is 15%.

Figure 1 shows a typical spectrum; over-all resolution obtained was 9 keV. Contaminant groups from two reactions appear in this figure. In addition, a group from the $^{13}\text{C}(d,t)^{12}\text{C}$ reaction was observed at larger angles. In order to minimize the effects of contaminants on the angular distributions, the angular interval was reduced from 5 to 3° forward of 30° laboratory angle. In this way the gaps in the angular distributions due to contaminants were kept small enough to prevent any l -transfer ambiguities. The upper limit on the excitation energy studied was 1.919 MeV, determined by the onset of the elastically scattered deuterons.

The spectra were reduced to angular distributions using the set of data-analysis computer programs written by Comfort.⁸ The uncertainty assigned to each point in the distributions is comprised of the statistical counting uncertainty, together with the uncertainties of background subtraction, doublet separation, and relative normalization. For most strong transitions this latter uncertainty, estimated to be $\pm 5\%$, dominates the error. The size of the data points in Figs. 2 to 5 represents an uncertainty of about $\pm 6\%$.

III. RESULTS AND DISCUSSION

A. Distorted-Wave Analysis

The measured angular distributions were compared to distorted-wave Born-approximation (DWBA) calculations made using the code DWUCK.⁹ The calculations were standard single-particle-transfer calculations. Both the finite range and nonlocal corrections available in DWUCK were employed. The values for the parameters used were those suggested for the (d,t) reaction in the instructions for use of the code⁹ ($\beta_d = 0.54$, $\beta_t = 0.25$, $R = 0.845$). The bound-state geometrical param-

TABLE II. Bound-state and optical-model parameters used in the DWBA calculations.

Source	V (MeV)	r_0 (fm)	a_0 (fm)	W (MeV)	$4W_D$ (MeV)	r_i (fm)	a_i (fm)	r_c (fm)	λ_{so}	
Bound states	...	a	1.17	0.75					25	
$^{87}\text{Rb} + d$	Ref. 10	90.3	1.2	0.75	...	49.2	1.33	0.72	1.15	...
$^{86}\text{Rb} + t$	Ref. 11	166.6	1.16	0.75	22.9	...	1.50	0.82	1.4	...

^a Adjusted to give correct separation energy.

ters are shown in Table II. The deuteron optical-model parameters used were those of Childs, Daehnick, and Spisak¹⁰ corresponding to 17.0-MeV deuteron scattering from ^{89}Y . The triton parameters were those of Flynn *et al.*,¹¹ corresponding to 20-MeV triton scattering from ^{90}Zr .

B. Levels with $l=4$ Angular Momentum Transfer

Figure 2 shows the angular distributions of those levels characterized by $l=4$ angular momentum transfer. The solid curves are DWBA predictions for $1g_{9/2}$ neutron pickup. The seven distributions shown actually represent eight levels, as the level labeled 0.556 MeV is known to be a doublet of states from previous (n, γ) work.⁶

It will be shown in following sections that the $3s_{1/2}$ and $2d_{5/2}$ neutron pickup strengths are quite small, and thus the $1g_{7/2}$ strength is presumably also quite small. Thus, to the extent that the ^{87}Rb ground state may be taken to be a pure $2p_{3/2}$ proton hole in ^{88}Sr , the spectroscopic factors listed in Table I for the levels shown in Fig. 2 can be directly interpreted as measures of the strengths of the component $(\pi p_{3/2}^{-1}, \nu g_{9/2}^{-1})$ in these levels. It can be seen from Table I and Fig. 6 that these seven transitions account for most of the $1g_{9/2}$ spectroscopic strength. The level at 1.412 MeV excitation was not observed in the previous (d, p) and (n, γ) studies.⁶ The absence of this level in these studies could presumably be accounted for by the purity of its proton configuration. This selectivity will be discussed further in Sec. IV.

C. Levels with $l=1$ Angular Momentum Transfer

Figure 3 shows the angular distributions of those levels characterized by $l=1$ angular momentum transfer. The solid curves are DWBA predictions for $2p_{3/2}$ neutron pickup. There is no J dependence expected or evident at these forward angles. However, from the known location of the $2p_{1/2}$ strength,¹² it is reasonable to expect that these 11 levels account for most of the $p_{1/2}$ and some of the $p_{3/2}$ spectroscopic strength. DWBA predictions for $2p_{1/2}$ transfer are 12% smaller than for the corresponding $2p_{3/2}$ transfer. Thus one can subtract the strength attributable to the $2p_{1/2}$ shell from the total strength represented by these 11 transitions, in order to get a measure of the $2p_{3/2}$ strength. The strength attributable to $2p_{3/2}$ is 1.6 particles out of 4.0 or about 40%. Such a percentage is consistent with the location of the $2p_{3/2}$ single-hole level relative to the $1g_{9/2}$ single-hole level in the $N=50$ core.¹²

The levels at 1.122, 1.156, and 1.762 MeV were not observed in the previously cited (d, p) and (n, γ) studies.⁶ Again, this could be accounted for by their $2p_{3/2}$ proton configuration. The strongly populated levels at 1.156 and 1.470 are interesting in that, despite their strength in this reaction, they are not populated at all in the $^{88}\text{Sr}(d, \alpha)^{86}\text{Rb}$ reaction.² This can be accounted for by the $\Delta T=0$ selection rule for (d, α) reactions, which together with data from the (n, γ) capture reaction, leads to unique assignments of $J^\pi = 0^+$ and 2^+ for these two levels. A more detailed discussion of these

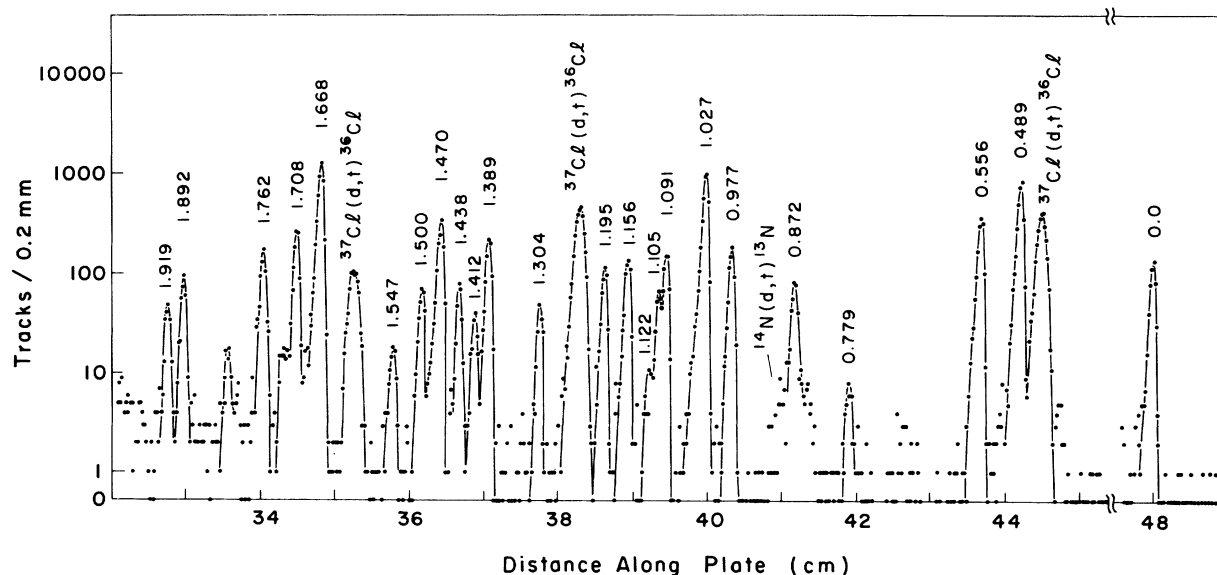


FIG. 1. Typical spectrum from the $^{87}\text{Rb}(d, t)^{86}\text{Rb}$ reaction at 17.5 MeV, at a lab angle of 18° . All the levels studied are evident in this spectrum except that at 1.245 MeV, which is obscured at this angle by a contaminant peak. The energy levels are labeled in MeV.

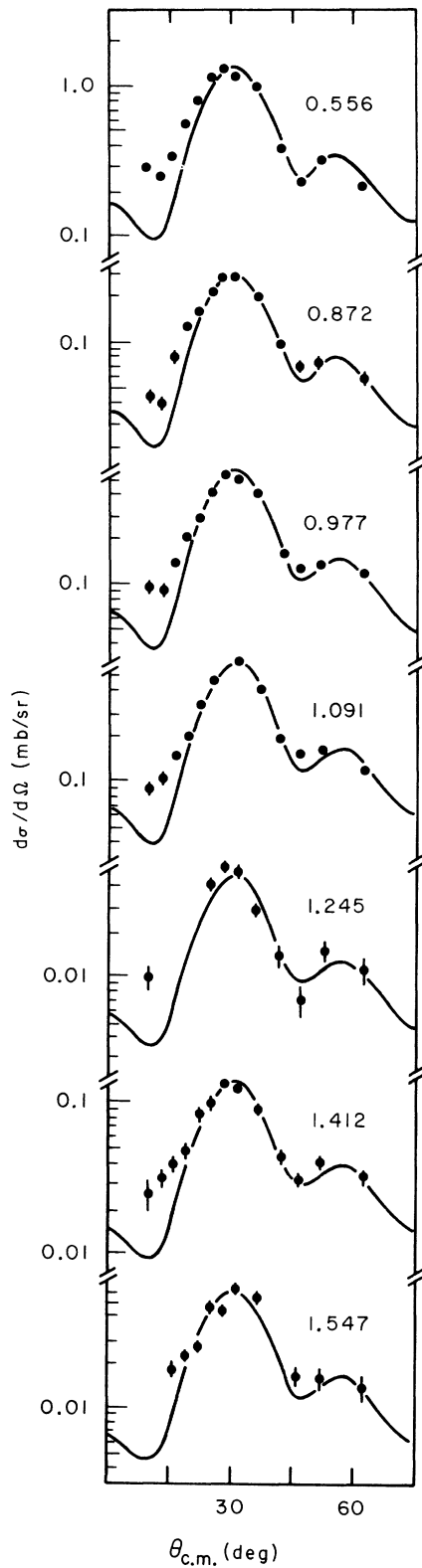


FIG. 2. Observed $l=4$ transfers in the $^{87}\text{Rb}(d,t)^{86}\text{Rb}$ reaction. The curves are DWBA predictions.

assignments is given in Ref. 2.

Because of the generally high quality of the DWBA fits, the discrepancies between the data and the $l=1$ curve for the level at 1.304 MeV are possibly significant. There was some evidence in Ref. 6 for a second level at 1.309 MeV; if this level exists, its expected $l=4$ angular distribution could account for the shape of the angular distribution of the 1.304-MeV level shown in Fig. 3.

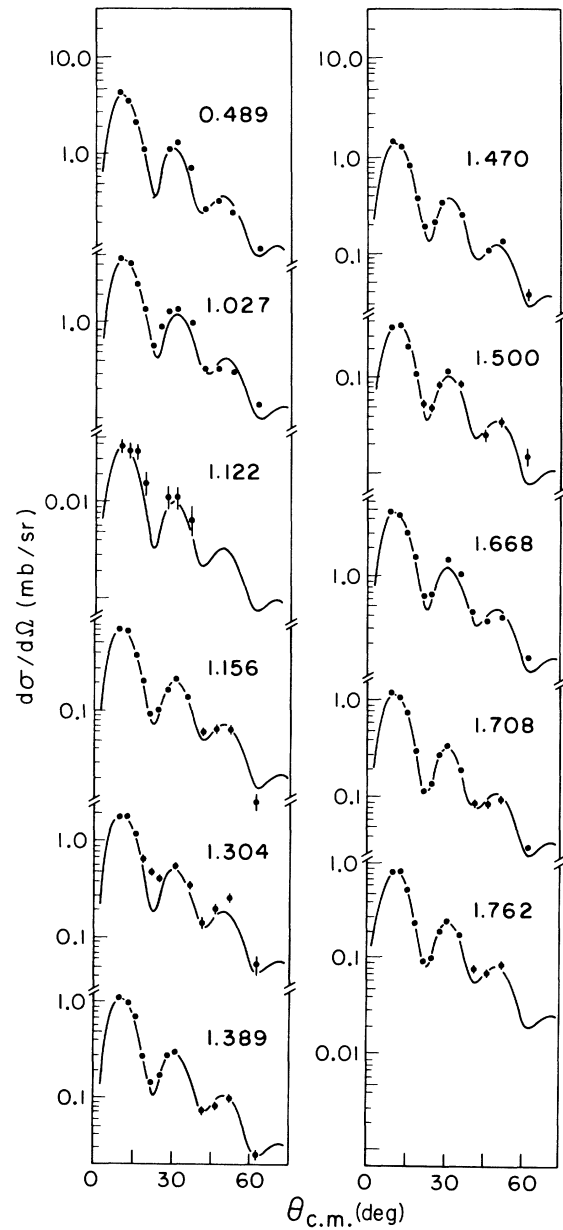


FIG. 3. Observed $l=1$ transitions in the $^{87}\text{Rb}(d,t)^{86}\text{Rb}$ reaction. The curves are DWBA predictions.

D. Levels with Mixed l Transfer

Figure 4 shows two angular distributions tentatively taken to be dominated by $l=3$ angular momentum transfer. The solid curves shown are DWBA predictions for $1f_{5/2}$ pickup, combined with a small mixture of $2p_{3/2}$ pickup required to fit the forward-angle data. The fit for the 1.105-MeV level is seen to be quite good, certainly sufficient to assign positive parity to that level. If the observed improvement of the fit at forward angles with the inclusion of the $l=1$ contribution is significant, the range of possible spins is reduced to $J^\pi = (1-3)^+$. The fit for the 1.892-MeV level is seen to be not as good; an increase in the relative $1f_{5/2}$ cross section, while improving the fit back of 30° , would tend to fill in the minimum at 22° and worsen the forward-angle fit. At first sight, the discrepancy between data and prediction would seem to suggest a doublet of states, excited by $l=1$ and $l=4$ transfer, respectively. However, the shapes of the $l=1$ and $l=4$ predictions are such that no combination of the two can reproduce the 22° minimum. In summary, although the $l=3$ plus $l=1$ mixture does not yield as good a fit for this 1.892-MeV level as for the 1.105-MeV level, it is better than that of any other

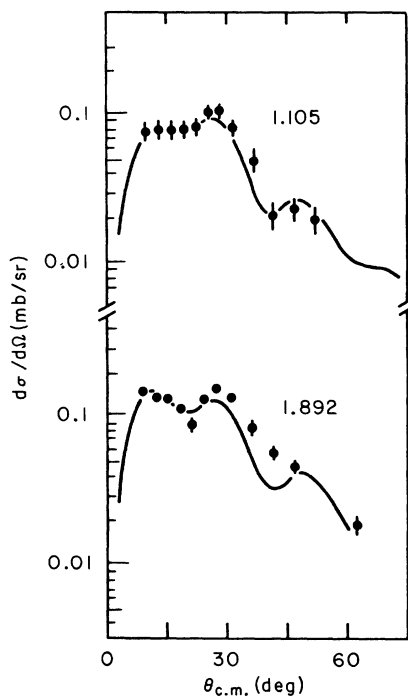


FIG. 4. Transitions characterized predominantly by $l=3$ angular momentum transfer. The difficulty of fitting the 1.892-MeV level may be evidence for a doublet of states at that energy.

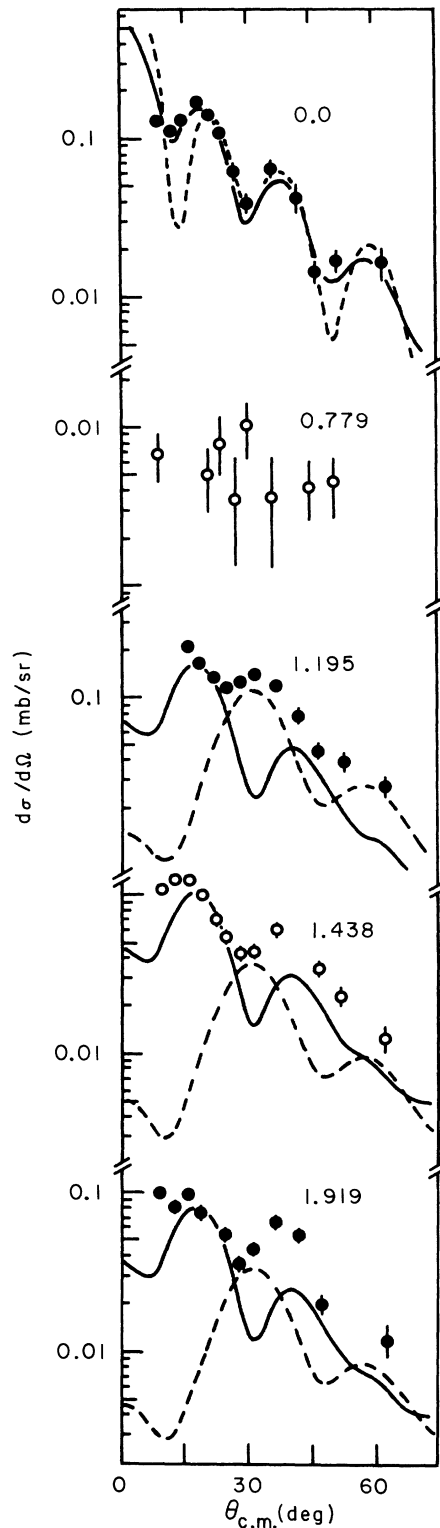


FIG. 5. Transitions to ^{86}Rb of uncertain angular momentum transfer. The various curves are described in the text.

combination of l values, including combinations permitting mixture of positive and negative parities. The relative strengths of $l=1$ and 3 used in the calculations shown in Fig. 4 are expressed in terms of spectroscopic factors in Table I. The combined $1f_{5/2}$ spectroscopic strengths of these two levels represent only 17% of the total $1f_{5/2}$ strength expected; however, due to the dynamic dominance of $l=1$ over $l=3$ transfer in the (d, t) reaction at 17.5 MeV, considerable $1f_{5/2}$ pickup strength could be hidden in the 11 $l=1$ transitions shown in Fig. 3.

E. Other Levels

Figure 5 shows the angular distributions of the remaining levels studied. Since ^{87}Sr has a closed $N=50$ neutron shell, the 2^- ^{86}Rb ground state is not expected to be excited in the simplest shell-model picture. The solid curve reproducing the observed cross section corresponds to a mixture of $l=0$ and $l=2$ transfers, indicating the presence of $3s_{1/2}$ and $2d_{5/2}$ neutrons in the target ground state. The spectroscopic factors extracted are listed in Table I. Due to the insensitivity of the fit to the precise mixture of the two configurations, the spectroscopic factors listed have large uncertainties. However, the order of magnitude is certainly correct, and shows the high sensi-

tivity of the (d, t) reaction for measuring this small imperfection in the $1g_{9/2}$ shell closure. The dashed curve shown for the ground state in Fig. 5 is the DWBA prediction for pure $3s_{1/2}$ pickup. Its failure to fit forward angles indicates the presence of a $2d_{5/2}$ component.

The level at 0.779 MeV was tentatively assigned $J^\pi = 7^-$ in Ref. 6. For this spin, there is again no single-step process in the simplest shell-model picture that will populate this level. The observed population could be accounted for in a number of ways, for example, by a weak higher-seniority component in the target ground state, or by a multistep process involving inelastic scattering. The extreme weakness of the 0.779-MeV level is in itself significant and is consistent with the $J^\pi = 7^-$ assignment for this level.

The three remaining levels shown in Fig. 5 could not be fitted by any single l calculation. However, the shapes of their angular distributions seem consistent with combinations of even l -value angular momentum transfers. The solid curve shown for these levels is the DWBA prediction for $2d_{5/2}$ pickup; the dashed curve that for $1g_{9/2}$ pickup.

IV. SUMMARY AND CONCLUSIONS

The levels of ^{86}Rb were studied by means of the (d, t) pickup reaction on the $\frac{3}{2}^-$ ground state of ^{87}Rb . 25 triton groups were observed up to an excitation of 1.92 MeV; four levels were observed for the first time in this experiment.

Distorted-wave calculations allowed a unique assignment of orbital angular momentum transfer to 18 of these groups. Seven were well fitted by $l=4$ calculations, and are interpreted as $1g_{9/2}$ pickup. These transitions account for all of the $1g_{9/2}$ spectroscopic strength. 11 angular distributions were well fitted by $l=1$ calculations. Based on the known single-hole level structure in the $N=50$ core,¹² these 11 levels were taken to include all the $2p_{1/2}$ spectroscopic strength. The remaining strength attributable to the $2p_{3/2}$ subshell then represents 40% of the total strength of that subshell.

Two levels were observed which seem to be characterized by $l=3$ angular momentum transfer. Together they represent only 17% of the total $1f_{5/2}$ subshell strength. This small number might be accounted for by the fact that, due to the dominance in this reaction of $l=1$ over $l=3$ transfer, some $1f_{5/2}$ strength could be mixed into the 11 $l=1$ transitions shown in Fig. 3, without affecting the quality of the pure $l=1$ fits.

The $J^\pi = 2^-$ ground state was excited with a mixture of $l=0$ and 2 angular momentum transfers, indicating a weak population of subshells outside

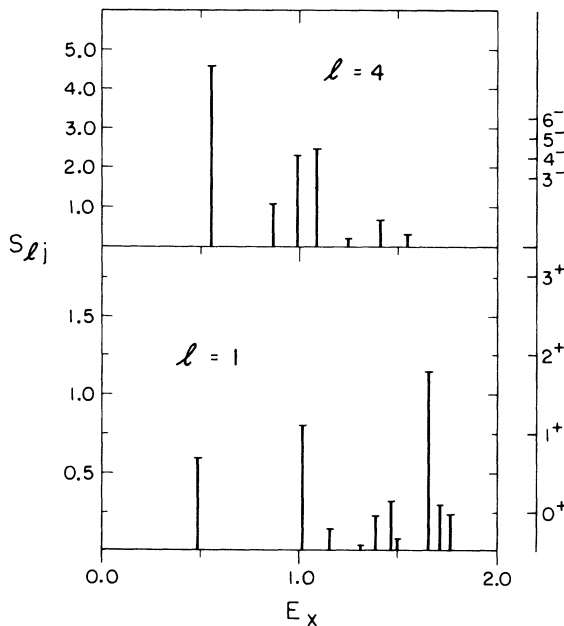


FIG. 6. Distribution of spectroscopic strengths for $l=4$ and 1 as a function of excitation energy. The scale at the extreme right represents the expected strength of the various members J^π of the multiplets formed by coupling the relevant neutron hole to a $2p_{3/2}$ proton hole.

the $1g_{9/2}$ subshell.

The ^{86}Rb levels at $E_x = 1.156$, 1.412 , and 1.762 MeV were strongly excited in the (d, t) reaction and yet were not observed in the (d, p) reaction.⁶ This selectivity could be accounted for by their proton configurations ($p_{3/2}$), which are different from that of the ^{85}Rb ground state ($f_{5/2}$).

It is interesting to consider the distribution of spectroscopic strength as a function of excitation energy. These distributions for $l=4$ and $l=1$ are shown in Fig. 6. For a pure $(\pi p_{3/2}^{-1}, \nu g_{9/2}^{-1})$ multiplet in ^{86}Rb one would predict $l=4$ population of four levels with $J^\pi = 3^- - 6^-$, each level having the spectroscopic factor shown at the right side of the figure. The excess strength to the level at 0.556 MeV supports the interpretation that both members of a known doublet are excited and that

one member is indeed the 6^- level. However, the remaining strength is fractionated over six other levels with excitation energies ranging up to 1.0 MeV away. For $l=1$, two levels are expected from the $(\pi p_{3/2}^{-1}, \nu p_{1/2}^{-1})$ configuration, and four from the $(\pi p_{3/2}^{-1}, \nu p_{3/2}^{-1})$ configuration. Figure 6 shows that 10 major states are seen instead of these six; in addition, measurable $l=1$ strength was found in three other levels not shown in the figure. Finally, the $l=1$ spectroscopic sums indicate that more $l=1$ states are expected above 2 MeV excitation. Therefore, although the assumption of single-neutron-hole configurations in the states of ^{86}Rb seems quite accurate, all observations indicate mixing of other proton configurations with the expected $2p_{3/2}^{-1}$ configuration.

*Work supported by the National Science Foundation.

¹See for example: M. R. Cates, J. B. Ball, and E. Newman, Phys. Rev. 187, 1682 (1969); T. S. Bhatia, W. W. Daehnick, and T. R. Canada, Phys. Rev. C 3, 1361 (1971).

²J. J. Kolata, W. W. Daehnick, and J. E. Holden, following paper, Phys. Rev. C 6, 1312 (1972).

³W. W. Daehnick, Phys. Rev. 177, 1763 (1969).

⁴J. R. Erskine and R. H. Vanderhohe, Nucl. Instr. Methods 81, 221 (1970).

⁵We are indebted to J. Childs for the use of his spectrograph focal-plane calibration code SPIRO.

⁶J. W. Dawson, R. K. Sheline, and E. T. Jurney, Phys. Rev. 181, 1618 (1969).

⁷G. Mairle and U. Schmidt-Rohr, Max Planck Institut für Kernphysik (Heidelberg) Report No. 1965 IV, 113 (unpublished).

⁸J. R. Comfort, ANL Physics Division Informal Report PHY-1970 B, 1970 (unpublished).

⁹P. D. Kunz, University of Colorado, distorted-wave Born-approximation computer code and instructions (unpublished).

¹⁰J. Childs, W. W. Daehnick, and M. Spisak, Bull. Am. Phys. Soc. 17, 446 (1972).

¹¹E. R. Flynn, D. D. Armstrong, J. G. Beery, and A. G. Blair, Phys. Rev. 182, 1113 (1969).

¹²H. Verheul, Nucl. Data A5, 457 (1972).